Biosensors and Bioelectronics: X 14 (2023) 100386

Contents lists available at ScienceDirect

Biosensors and Bioelectronics: X

journal homepage: www.journals.elsevier.com/biosensors-and-bioelectronics-x

Development of electrochemical immunosensor for quantitative detection of non-small cell lung cancer (NSCLC) biomaker YES1

Lucia K. Kiio [a,b,c,*], John O. Onyatta [b], Peter M. Ndangili [c], Florence Oloo [c], Carolina Santamaría [d], Luis M. Montuenga [a,e,f,g], Damaris N. Mbui [b]

[a] Program in Solid Tumors, Centro de Investigación Médica Aplicada (CIMA), University of Navarra, 31008, Pamplona, Spain
[b] Department of Chemistry, University of Nairobi, 30197, 00100, Nairobi, Kenya
[c] School of Chemistry and Material Science, The Technical University of Kenya, 52428, 00200, Nairobi, Kenya
[d] BIOMA Center, Department of Chemistry, School of Sciences University of Navarra, Irunlarrea,1, 31008, Pamplona Spain
[e] Department of Pathology, Anatomy and Physiology, School of Medicine, University of Navarra, Pamplona, Spain
[f] Consorcio de Investigación Biomédica en Red de Cáncer (CIBERONC), Madrid, Spain
[g] Navarra Health Research Institute (IDISNA), Pamplona, Spain

ARTICLE INFO

Keywords:
Electrochemical immunosensor
Non-small cell lung cancer
Thiolated protein G
Voltammetry
YES1

ABSTRACT

Non-small cell lung cancer (NSCLC) is the most common type of lung cancer accounting for 85% of all newly diagnosed cases. Its prognosis remains poor as most patients are diagnosed at an advanced stage. In this study, we report the development of an electrochemical immunosensor for quantitative detection of Yamaguchi sarcoma viral oncogene homolog 1 (v-YES1) protein, comprised of a glassy carbon electrode modified with gold nanoparticles (AuNP), thiolated protein G (TPG), YES1 antibody (AB1) and glutaraldehyde (GA), which was used as a cross linker. Cyclic voltammetry (CV) and Differential pulse voltammetry (DPV) were used to measure the response and characterization of the fabricated immunosensor. The fabricated immunosensor, glassy carbon electrode (GCE)/AuNP/TPG/GA/Ab1) was optimized for pH, response time, antibody concentration and temperature. Under optimum conditions, the immunosensor displayed high sensitivity, recording a limit of detection (LOD) of 0.0014 ng/mL and was noted to have negligible cross reactivity. The proposed immunosensor proved to be stable for up to 2 weeks, which means that it can be used as an alternative diagnostic tool for the rapid, sensitive and specific detection of YES1 antigen in clinical samples for clinical monitoring of cancer progression.

1. Introduction

The most common type of lung cancer is the non-small cell lung cancer (NSCLC) accounting for 85% of all newly diagnosed cases (Chen et al., 2021).

The histology of NSCLC classification follows the 2015 World Health Organization (WHO) classification of lung tumors. The classification system relies on immunohistochemistry and light microscopy in order to better guide the treatment and determine a prognostic course. NSCLC includes various lung cancers like adenocarcinoma, squamous cell carcinoma, and large cell carcinoma. Adenocarcinoma originates from glandular cells of bronchial mucosa and represents the dominant histological subtype among the other lung cancer types. Squamous lung cancer arises from the modified bronchial epithelial cells and is characterized by keratinization, keratin pearl formation or the presence of intercellular bridges (Travis, 2012).

Most lung cancer patients are diagnosed at an advanced stage and therefore, their prognosis remains poor despite recent progress in chemotherapeutic treatments (Wang et al., 2017). Detection at an early stage is of profound importance in cancer treatment and may save millions of lives (Gong et al., 2019). Thus, early cancer detection techniques, preferably those that are non-invasive or minimally invasive like CT-based screening have been developed and implemented (Adams et al., 2023). As a way of optimizing imaging-based screening, validated biomarkers need to be developed (Seijo et al., 2019). Liquid biopsy, which evaluates molecular markers in biological fluids such as plasma (Michela, 2021), saliva (Patel et al., 2022) or urine (Jain et al., 2019) may be useful for cancer detection. These minimally invasive or non-invasive diagnostic techniques enable rapid sampling and real-time repeatable detection.

* Corresponding author. Program in Solid Tumors, Centro de Investigación Médica Aplicada (CIMA), University of Navarra, 31008, Pamplona, Spain.
E-mail address: lucy.k630@tukenya.ac.ke (L.K. Kiio).

https://doi.org/10.1016/j.biosx.2023.100386
Received 29 November 2022; Received in revised form 2 April 2023; Accepted 21 April 2023
Available online 9 August 2023

YES1 is a member of the Src kinase family of proteins. The YES1 protein is an important NSCLC tumor marker. Studies by (Garmendia et al., 2019) showed that high YES1 levels or gene amplification are significantly associated with shorter overall survival in patients with NSCLC. Garmendia et al. (2019) and Redin et al. (2021) have shown that YES1 levels can be a good companion biomarker for predicting the tumor response to Dasatinib, a Src kinase inhibitor or to more specific YES1 inhibitors.

YES1 could therefore, be an important biomarker for clinical management of lung cancer. Immunohistochemistry (Cha et al., 2021), western blotting (Takeda et al., 2017), flow cytometry and quantitative real-time polymerase chain reaction (QRTPCR) (Garmendia et al., 2019) are some of the molecular techniques which have been employed to detect YES1. However, some of these techniques can be cumbersome, time-consuming or relatively expensive in terms of reagents.

An alternative method of detection could entail the use of electrochemical immunosensor, which has distinct advantages, such as high selectivity (Jing et al., 2020), faster response, low sample requirements, miniaturization and excellent sensitivity (Zhang et al., 2019; Lv et al., 2018).

To date, there has been no documented attempt to develop an immunosensor for the detection of YES1. In this study, electrochemical immunosensor for the detection of YES1 expression in NSCLC has been developed. Gold nanoparticles and thiolated protein G were used as the matrix support for antibody immobilization on a GCE surface. Gold nanoparticles have been widely used to develop various biosensors because of their excellent prospects for chemical and biological sensing (Fatima et al., 2022). They also provide a suitable platform for multifunctionalization with a wide range of organic or biological ligands for selective detection of biomarkers (Yakoh et al., 2015). In the present study, recombinant human YES1 was used as the target protein, and polyclonal anti-YES1 antibody as the bio-recognition molecule. YES1 antibody was preferred over aptamers and peptides because of its reusability, selectivity and its stability in biological media unlike aptamers, which are prone to quick degradation in biological media due to interactions with biomolecules and also associated with non-specific binding (Morales and Halpern, 2018).

The ability of the developed immunosensor to quantify YES1 in real samples was evaluated using cell culture supernatant and cell lysates of cultured human lung cancer cell lines, H2009, A549, H2170 and H23. The immunosensor had a wide detection range, low detection limit and provided basis for a design strategy which can be used in the detection of other biomarkers in clinical setting.

2. Materials and methods

The details of instruments and reagents used are described in the online supplementary material and methods.

2.1. Cell culturing, maintenance of human cell lines

The details of the methodology used are described in the online supplementary material and methods.

2.2. Concentration of cell culture supernatants

Amicons of molecular weight cut-off 3 kDa and 10 kDa sizes were used for maximum sample recovery of concentrated cell culture supernatant. Ultra-4 Amicon was filled with up to 4 mL media volume ensuring that the screw closure was fully sealed. The supernatant was centrifuged for 30 min at 4000 rpm at 4 °C using a swing bucket centrifuge type. The filtrate container was emptied and the concentrator tube refilled with additional sample and the centrifuge process was repeated until all the sample was loaded.

2.3. Detection of YES1 expression in cell lines and antigen characterization

The details of the methodology used are described in the online supplementary material and methods.

2.4. Fabrication principle of electrochemical immunosensor, optimization and electrochemical measurement

A glassy carbon electrode was mechanically cleaned and electrochemically treated by cycling the potential between −0.4V and +1.0 V in 0.1 M H_2SO_4. Gold nanoparticles (AuNPs) were electrodeposited onto the electrode surface using cyclic voltammetry for 25 cycles at a potential range of - 0.4 V–1.0 V in 1 mM gold tetrachloride acid trihydrate ($HAuCl_4 \cdot 3H_2O$) and 0.1 M hydrochloric acid (HCl). 15 μL of 20 mM TPG was drop coated onto the modified electrode (GCE/AuNP) for 4 h at 4 °C. After washing with ultrapure water, this electrode (GCE/AuNP/TPG) was incubated for 1 h by placing it in 15 μL of 4% GA at room temperature. The modified electrode was thoroughly washed with sterile deionized water to remove any loosely bound glutaraldehyde. Subsequently, the surface of the electrode (GCE/AuNP/TPG/GA) was covered with 10 μL of polyclonal rabbit YES1 antibody by drop casting, and then incubated overnight at 4 °C. The surface of the modified electrode was rinsed with tween buffer to remove any unbound antibody. Finally, to circumvent any nonspecific binding, the modified electrode (GCE/AuNP/TPG/GA/Ab1) was blocked with 10 μL of (3%) BSA. This completed the fabrication of the immunosensor, and was stored at 4 °C in phosphate buffer solution (PBS) pH 7.2 when not in use. For electrochemical characterization, saturated Ag/AgCl was used as the reference and platinum as the counter electrode.

This was done by CV sweeping the potential from −0.7 V to 0.3 V and from −0.5 V to 0.1 V when Differential Pulse Voltammetry (DPV) was done both in K_3 $[Fe(CN)_6]$ solution using a scan rate of 50 mV s^{-1}. In order to obtain maximum sensing signal of YES1-Ab on the GCE/AuNP/TPG/GA electrode various factors such as pH, Ab concentration, GA concentration, incubation time and temperature were optimized by comparing DPV data.

Electrochemical measurements with the GCE/AuNP/TPG/GA/Ab1/BSA electrode were done by incubating the electrode in solutions with various concentrations (0.01 ng/mL to 100 ng/mL) of YES1 antigen for 30 min at 37 °C. It was then, washed with tween buffer X 1 solution, and dried under a nitrogen steam. The electrode was then immersed in secondary horseradish peroxidase (HRP) conjugated anti-rabbit (Ab2-HRP) solution for the sandwich immunoreaction, after which it was cleaned using 0.01 M PBS and then dried using nitrogen gas. DPV was performed at a potential range of −0.4V–0.1V at a scan rate of 50 mV s^{-1}.

The factors of the fabricated GCE/AuNP/TPG/GA/Ab1 sensor that were investigated include: limit of detection (LOD), degree of cross reactivity, repeatability and stability for a period of 2 weeks and its specificity against other compounds that had a possibility of interfering with YES1 in human environment.

3. Results and discussion

3.1. Design and fabrication principle of GCE/AuNP/TPG/GA/Ab1 based immunosensor

Fig. 1 elucidates the fabrication principle of the developed GCE/AuNP/TPG/GA/AB1/BSA immunosensor. The AuNPs provided a large surface area for the immobilization of capture antibody and also amplified the electrochemical signal by enhancement of electrical conductivity.

Presence of AuNPs served as a platform for the attachment of TPG where thiol sites of the L-cysteine were chemisorbed on the surface of the GCE/AuNp. GA acted as a cross linker of the antibody with the

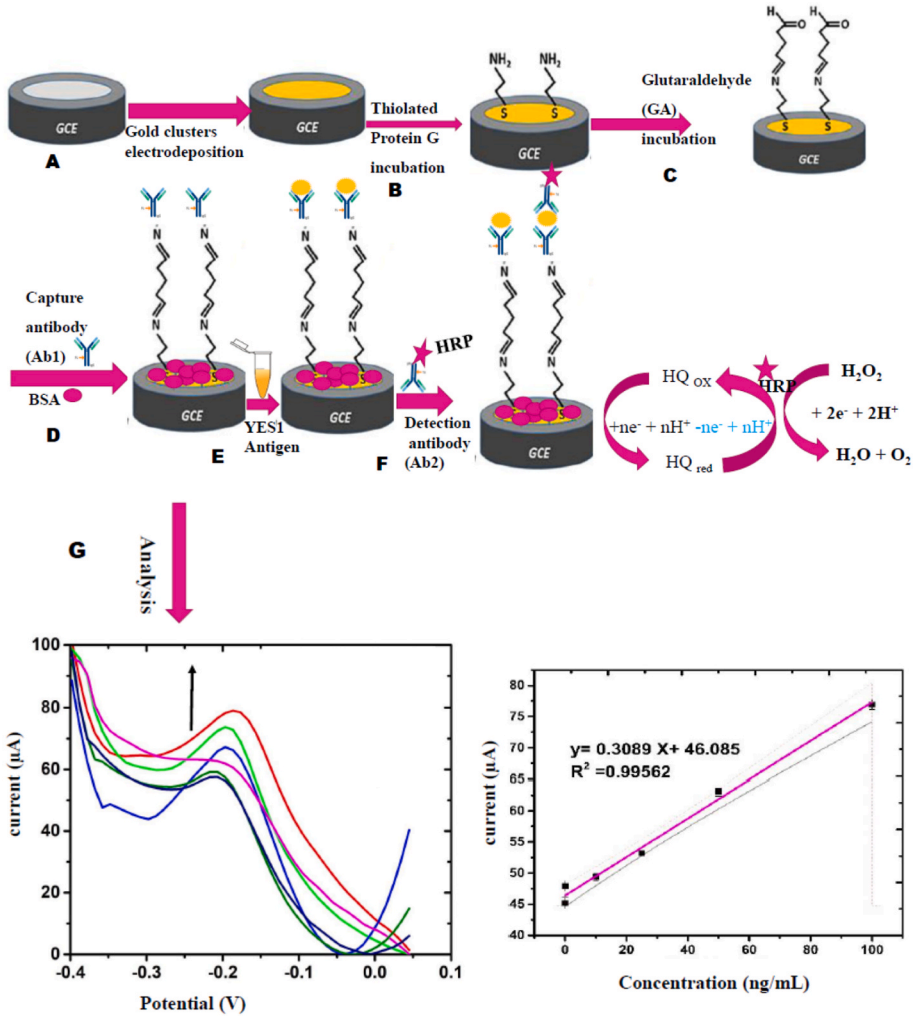

Fig. 1. Schematic presentation procedure for the preparation of GCE/AuNP/PTG/GA/Ab1 BSA immunosensor and electrochemical measurement of YES1 antigen; (A) Bare GCE and electrodeposition of AuNPs of the electrode surface; (B) Incubation of GCE/AuNPs with thiolated protein G (TPG); (C) Addition of GA to cross link the capture antibody; (D) Immobilization of YES1 antibody on GCE/AuNPs/TPG/GA surface via covalent binding; antibody blocking using BSA; (E) Incubation with analyte containing YES1 antigen; (F) Incubation with detection antibody labeled with HRP; (G) Electrochemical detection.

thiolated protein G. Addition of YES1 Ab on GCE/AuNP/TPG/GA allowed the incorporation of the antibody to the modified electrode. The immobilization reaction was based on formation of an amine group following the reaction between the aldehyde group of glutaraldehyde and the YES1 antibody. The orientation and polarity of the protein molecules played a crucial role in the electron transfer from the electrode surface, and subsequent enhancement of an electric current.

3.2. Characterization of the proposed immunosensor and cyclic voltammetric characteristics of the system

CV and DPV were used to characterize the surface of the electrode after each modification. The results obtained were consistent with those of Layqah and Eissa (2019) and Tran et al. (2019).

The Cyclic Voltammograms of (a) GCE (b) GCE/AuNP (c) GCE/AuNP/Thiolated protein G (TPG) (d) GCE/AuNP/TPG/GA (e) GCE/AuNP/TPG/GA/Ab1 (f) GCE/AuNP/TPG/GA/Ab1/BSA electrodes are presented in Fig. 2 and S1 (A).

After the Au-nanoparticles were deposited on the GCE, the peak heights of the redox couple were observed to increase considerably, owing to the enlarged surface area of the electrode and the improved rate of electron transfer (Fig. 2 and S1A). The peak heights of the redox couple also increased after the incubation with the TPG on the GCE/AuNP electrode due to the electrostatic interaction and attraction between the $[Fe(CN)_6]^{3-}$ and the amine terminals of the GCE/AuNP/TPG modified electrode. The peak heights decreased when GA, YES1 antibody and BSA were added onto the GCE/AuNP/TPG modified electrode.

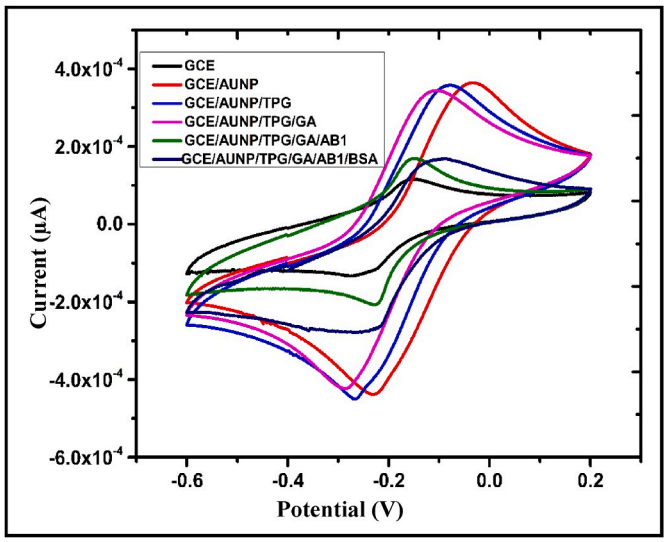

Fig. 2. Characterization of the electrochemical performance of the modified electrode cyclic voltammetry curves recorded in 5 mM $K_3[Fe(CN)^6]$ and 01. M KCl at a scan rate of 50 $mVs^{-1.}$

This was attributed to the non-conductivity of GA, Ab1 and BSA. The electroactive area of GCE/AuNPs was calculated according to the Randles–Sevcik equation (Hill and Kelley, 2008). The electroactive surface area of bare GCE, GCE/AuNP and GCE/AuNP/TPG modified electrodes was calculated as 0.01438 cm^2, 0.0664 cm^2 and 0.02659 cm^2 respectively and the results indicated an improved electrochemical activity over the modification of bare GCE by GCE/AuNP and GCE/AuNP/TPG. The results were consistent with previous studies, for instance, the effective surface areas of poly (4-amino-

3-hydroxynaphthalene sulfonic acid) modified glassy carbon electrode (PGCE) and activated glassy carbon electrode (AGCE) were calculated to be 0.037 and 0.027 cm^2, respectively, for potentiodynamic fabrication and characterization for both modified electrodes (Amare and Admassie, 2020).

CV scans were performed at increasing scan rates ranging from 10 to 100 mV s^{-1} in a bid to determine the mode of electron transfer. It was realized that the redox reactions (for both Ipa and Ipc) increased linearly with increasing scan rate (Fig. S1B), showing that the electrochemical signal was due to diffusion-controlled surface reaction. The ultimate linear equations determined for Ipa were $y = 1.533 \times 10^{-5} x + 3.162 \times 10^{-5}$; ($R^2 = 0.9926$) and for Ipc: $y = 1.2339 \times -4 x10^{-5}$; ($R^2 = 0.9924$) (Fig. S1C).

The linearity of both equations demonstrated that the electrochemical signal was due to diffusion-controlled surface reaction. Characterization of YES1 protein showed that its molecular weight was approximately 60 kDa (Fig. S1D).

3.3. Optimization of developed GCE/AuNP/TPG/GA/Ab1 based immunosensor

Investigation of changes in peak current with pH variation from 6.2 to 7.6 showed that the current increased from 6.2 up to 7.2 after which there was a subsequent decrease (Fig. S2A). This was consistent with the pH of body fluid, meaning that antigens and antibodies were able to maintain their bioactivity at a near-neutral pH. Therefore, pH 7.2 was used for the PBS solution in subsequent reactions. Investigation of effect of incubation time of the analyte (rYES1 solution) at 37 °C on reaction rate showed that the current for YES1 detection increased as time increased up to 30 min and there was no further increase, indicating that the captured YES1 antigen had reached saturation (Fig. S2B). Therefore, 30 min incubation time was taken as the optimum time for experiments.

The effect of antibody concentration of YES1 (0.099 mg/mL) on the performance of the immunosensor, when the dilution ratio was varied from 1:200 to 1:2000 showed that the oxidation current increased from 1:200 to 1:500 after which the current decreased (Fig. S2C). Therefore, a dilution of 1:500 was selected as the optimum dilution ratio of YES 1 antibody.

Incubation of GCE/AuNP/TPG modified electrode in solutions containing different concentrations of GA at room temperature for 3 h showed that the concentrations of 4% and 5% had better responses of the immunosensor towards YES1 than the 3% concentration. Therefore 4% was chosen to be the optimum GA dilution (Figs. S2D and E).

The standard calibration curve was plotted based on Fig. 3 and a linear regression equation was calculated as $y = 0.3089X + 46.085$ (Fig. S3A). The limit of detection (LOD) and limit of quantification (LOQ) of the immunosensor were calculated from the expressions LOD = (3X SD/m) and LOQ = (10X SD/m) (Armbruster and Pry, 2008), where **SD** is the estimated standard deviation of the data and **m** is the slope. The LOD and LOQ obtained were 0.0014 ng/mL and 0.0046 ng/mL respectively. The detection limit obtained with the developed immunosensor was lower than the reported immunosensor for other cancer biomarkers (Table 2) provided in the online supplementary material.

To investigate whether the detection of the oxidation peak was a valid means of assessing the concentration of YES1 in cells, different amounts of A549 cells were assessed using the developed immunosensor. It was observed that when the number of cells were gradually increased from 100 to 500,000, the oxidation peaks current increased significantly (Fig. S3B), suggesting that the limit of detection of the sensor could be less than 100 cells. Western blot analysis was used to verify the results of the immunosensor (Fig. S3C).

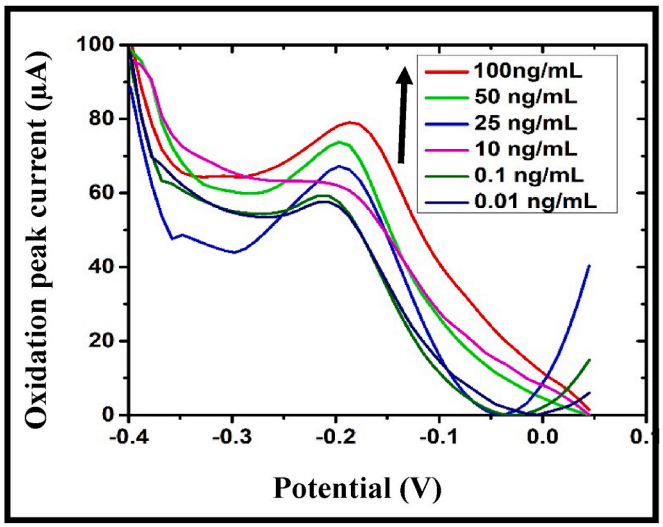

Fig. 3. DPV detection at varying YES 1 concentration (0.01–100 ng/mL) in 0.1 M PBS (pH 7.4) with 5 mM [$K_3Fe(CN)_6$, 0.1 M KCl and 4 mM H_2O_2. Scan rate: 50 mV s^{-1}.

Table 1
Antibodies used for western blotting
Antibodies and concentration that were used were as indicated in Table 1 β-actin was used as the loading control.

Antibody	Name of antibody	Company	Species	Dilution
Primary Antibody				
	YES 1	Cell signaling	Rabbit	1: 1000
	β- actin	Sigma- Aldrich	Mouse	1: 1000
Secondary Antibody				
	Anti- IgG Rabbit-HRP	Thermo Fisher Scientific	Sheep	1: 2000

3.4. Analytical performance of the developed GCE/AuNP/TPG/GA/Ab1 based immunosensor

The analytical performance of the proposed GCE/AuNP/TPG/GA/Ab1 immunosensor was evaluated at the protein level using DPV measurements which showed that the peak current signals of YES1 increased with increasing concentrations of YES1 protein ranging from 0.01 ng/mL to 100 ng/mL (Fig. 3).

The obtained results showed that the developed immunosensor has an acceptable analytical performance and also that it is responsive to YES1 even at very low concentrations.

Western blotting of cell lysates and supernatants of A549, H2009, H2170 and H23 cell lines confirmed that the immunosensor can be used to detect YES1 not only in A549 cells but also in the cultured cell supernatants of other cell lines such as H2009, H23 and H2170 (Figs. S3D and E). The results obtained using the proposed immunosensor were also verified using immunoblotting (Figs. S3F and G)

Table 2
Comparison of the response characteristics of different modified electrodes.

Electrode	Target biomarker	Detection range	Detection limit	Method	Ref
GCE/AuNP/TPG G/GA/Ab1/BSA	YES1	0.01–100 ng/mL	0.001408 ng/mL	DPV	This work
FTO/SWCNTs/den-Au/prob	miR-21	0.01 fM L^{-1} - 1 μM L^{-1}	0.01 fM L^{-1}	DPV	Sabahi et al. (2020)
GCE/G2Fc/Ab	IgG	5.0–50 ng/mL	2.0 ng/mL	DPV	(Khanmohammadi et al., 2020)
Dye labeled DNA probe	CA15-3	0.01–1 U/mL	0.0039 U/mL	A.C impedance	Zhao et al. (2020)
Self-assembled ferrocenecored poly (amido amine) dendrimers	BRCA1	1.3–20 nM	0.38 nM		Senel et al. (2019)
ERBB2c modified probe CD24c DNA modified probe	HER2	0.37–10 nM	0.16 nM 0.23 nM	Electrochemical impedance spectroscopy	Saeed et al. (2017)
ssDNA modified prob	CYFRA21-1	10 fM – 100 nM	1.0×10^{-14} M	DPV	(Chen et al., 2018)
Fe_2N NPs@rGOS/prob	4-NQO	0.05–574.2 μM	9.24 nM		(Chen et al., 2020)
p53-Ab2-tGO-AuNPs	p53	20 - 1000 fg/ml	4 fg/ml	electrochemical impedance spectroscopy (EIS)	(Aydın and Sezgintürk, 2017)
ssDNA λ-exo modified prob	EGFR exon 21	0.1 μM–3 μM	120 nM	DPV	Shoja et al. (2018)

3.5. Reproducibility, storage stability and cross reactivity of the immunosensor

3.5.1. Storage stability

The stability of the GCE/AuNP/TPG/GA/Ab1 fabricated electrode was used to check its response towards 50 ng/mL of YES1. This immunosensor was stored in PBS (0.1 M, pH 7.2) at 4 °C up to 15 days and only a slight decrease in signal was seen at the 15th day (Fig. S4). The immunosensor was found to retain 95.5% of the original electrochemical signal and a relative standard deviation (RSD) of 3.1%. The storage stability for the developed immunosensor was acceptable compared to the immunosensors reported previously from studies such as that of Jing et al. (2020), for an electrochemical immunosensor developed for sensitive detection of the tumor marker carcinoembryonic antigen (CEA) based on three-dimensional porous Nano platinum/-graphene where the electric signal retained was 96% after two weeks. Results obtained for ultrasensitive multiplexed immunoassay of autophagic biomarkers based on Au/rGO and Au nano cages amplifying electrochemical signal showed that the storage stability of the biosensor was 91.5% after two weeks (Wang et al., 2017).

3.5.2. Reproducibility of the immunosensor

Reproducibility of the immunosensor was evaluated for GCE/AuNP/TPG/GA/Ab1 fabricated electrode. In this case, multiple readings of 10 ng/mL of YES1 were analyzed using freshly prepared immunosensors (Fig. S5A). The results indicated that each individual electrode could be used up to 6 times without major changes in the peak current. After the 5th time, a drop in current was observed which meant that most of the immobilized YES1 on the surface of the immunosensor may have been removed due to multiple rounds of washing. The relative standard deviation (RSD) value obtained from the six experiments was calculated to be 5.2%. This is comparable to other studies, for example the RSD of an immunosensor for sensitive detection of CEA based on three-dimensional porous Nano platinum/graphene peak current was found to be 5.1% (Jing et al., 2020) while RSD for quantitative detection of breast cancer biomarker UBE2C was 3.11% (Jayanthi et al., 2019).

Assessment of reproducibility was also done using four identically prepared GCE/AuNP/TPG/GA/Ab1 electrodes and placing each of them in the prepared 10 ng/mL YES1 solution, and recording the DPV signal. The results obtained revealed that a relative standard deviation (RSD) of 2.7% was obtained (Fig. S5B). These results compared well with the results obtained in the literature, for instance, for an immunosensor prepared for detection of UBE2C the observed RSD was 3.51% (Jayanthi et al., 2019). This indicated that the developed immunosensor possessed an acceptable precision and reproducibility since differently assessed immunosensors gave similar results.

3.5.3. Cross reactivity

Evaluation of cross reactivity of the immunosensor was done using several compounds that had a possibility of interfering with YES1 in the human environment. The compounds introduced consisted of actin, BSA, glyceraldehyde-3-phosphate dehydrogenase (GAPDH), vascular endothelial growth factor (VEGF) and L-cysteine. The developed immunosensor was incubated in a solution of 10 ng/mL rYES1 containing each of the above-mentioned compounds (100 ng/mL). The results (Fig. S6) indicated that the change in current caused by the interfering compound was less than 3.0% when compared to situations where there was no interference, indicating that the immunosensor had good selectivity. The immunosensor showed better performance compared to the results previously reported in literature for instance, in the immunosensor for sensitive detection of CEA based on three-dimensional porous nano platinum/graphene the change in current caused by interfering compound was less than 5.4% compared to results with no interference present (Jing et al., 2020). The electro catalytic current response was less than 5% of that without the interference in the case of the ultrasensitive sandwich-type electrochemical immunosensor for detection of CEA based on tri-metallic nanocomposite (Tian et al., 2016).

3.6. Detection of YES1 in human plasma samples

The recoveries of the spiked samples varied in the range of 97.5%–110%. The RSD was obtained in the range of 0.35%–7.26%. Comparison of RSD results obtained in this study with similar immunosensors showed that the fabricated immunosensors compared well for example with the recovery values and RSD of electrochemical immunosensors for diagnosing COVI-19 which were in the range of 96.97%–101.9% and 4.99%–5.74% respectively (Liv, 2021). Jayanthi et al. (2019) reported results for an immunosensor developed for detection of UBE2C, which had recovery values and RSD in the range of 89.72%–103.76% and 1.297%–4.201% respectively. The results showed that the fabricated immunosensor had significant potential for detecting YES1 in real plasma samples; Table 3 provided in the online supplementary material.

4. Conclusions

In this proposed study we successfully developed GCE/AuNPs/TPG/GA/YES1-Ab modified electrode for rapid detection of YES1 protein with LOD of 0.0014 ng/mL in standard buffer. The developed immunosensor showed no cross reactivity with any possible interfering compounds with YES1 in human environment. It had a rapid response time of 8 s, with a storage shelf life of 2 weeks. The only limitation of the immunosensor was the need for a potentiostat for evaluating the current

Table 3
Detection of YES1 in human plasma samples.

Sample no.	YES1 recombinant added (ng/mL)	YES1 found by immunosensor (ng/mL)	Total YES1 found by immunosensor	Recovery (%)	Relative Standard Deviation RSD (%)
1	0.1	39.02	40.01	99	1.77
2	1.0	22.00	22.11	110	0.35
3	10.0	90.15	99.90	97.5	7.26

readings of the electrode, which may be considered to be bulky. Nevertheless, it is easy to fabricate and requires less time compared to the gold standard ELISA technique. Furthermore, since the glassy carbon electrodes were obtained locally, the overall cost of the electrode fabrication reduced substantially making it a cheaper alternative. The sensor also shows great future research prospective for detection of several other diseases since it can easily be customized by immobilizing any bio-receptor onto the GCE/AuNPs/TPG, specific to a particular target analyte. Moreover, the immunosensor could be miniaturized in order to develop a point of care gadget that can be used for clinical monitoring of cancer progression.

Funding

This work was supported by CIMA and University of Navarra; Fundación Ramón Areces, Spanish Ministry of Economy and Innovation and Fondo de Investigación Sanitaria-Fondo Europeo de Desarrollo Regional (PI19/00098) and Fundación Roberto Arnal Planelles, Gandhi Smarak Nidhi fund post graduate scholarship and Harambee Africa, Guadalupe scholarship program for African researchers.

CRediT authorship contribution statement

Lucia K. Kiio: Conceptualization, Methodology, Software, Formal analysis, Investigation, Writing – original draft, Data curation, Funding acquisition. **John O. Onyatta:** Conceptualization, Methodology, Data curation, Visualization, Validation, Writing – review & editing, Visualization, Supervision. **Peter M. Ndangili:** Conceptualization, Methodology, Validation, Visualization, Data curation, Writing – review & editing, Visualization, Supervision. **Florence Oloo:** Writing – review & editing, Resources, Visualization. **Carolina Santamaría:** Conceptualization, Methodology, Writing – review & editing, Resources, Visualization. **Luis M. Montuenga:** Conceptualization, Methodology, Writing – review & editing, Resources, Visualization, Validation. **Damaris N. Mbui:** Conceptualization, Methodology, Validation, Visualization, Data curation, Writing – review & editing, Visualization, Supervision, Project administration.

Declaration of competing interest

The authors declare that they have no known competing financial interests or personal relationships that could have appeared to influence the work reported in this paper.

Data availability

Data will be made available on request.

Acknowledgements

This work was supported by FIMA, CIBERONC (CB16/12/00443), Spanish Ministry of Economy and Innovation and Fondo de Investigación Sanitaria-Fondo Europeo de Desarrollo Regional (PI22/00451).

Appendix A. Supplementary data

Supplementary data to this article can be found online at https://doi.org/10.1016/j.biosx.2023.100386.

References

Adams, S.J., Stone, E., Baldwin, D.R., Vliegenthart, R., Lee, P., Fintelmann, F.J., 2023. Lancet 40110374, 390–408.
Amare, M., Admassie, S., 2020. J. Mater. Res. Technol. 9, 11484–11496.
Armbruster, D.A., Pry, T., 2008. Clin. Biochem. Rev. 29 (Suppl. 1), S49–S52.
Aydın, E.B., Sezgintürk, M.K., 2017. Talanta 172, 162–170.
Cha, Y.J., Bae, S.J., Kim, D., Ahn, S.G., Jeong, J., Koo, J.S., Yoo, T.-K., Park, W.-C., Lee, A., Yoon, C.I., 2021. Front. Oncol. 11, 609743.
Chen, T.-W., Tamilalagan, E., Chen, S.-M., Akilarasan, M., Maheshwaran, S., Liu, X., 2020. Int. J. Mol. Sci. 21 (9), 3273.
Chen, M., Wang, Y., Su, H., Mao, L., Jiang, X., Zhang, T., Dai, X., 2018. Sensor. Actuator. B Chem. 255, 2910–2918.
Chen, M., Wu, D., Tu, S., Yang, C., Chen, D., Xu, Y., 2021. Sci. Rep. 11.
Fatima, A., Younas, I., Ali, M.W., 2022. Arch. Pharm. Pract. 13, 5–10.
Garmendia, I., Pajares, M.J., Hermida-Prado, F., Ajona, D., Bértolo, C., Sainz, C., Lavín, A., Remírez, A.B., Valencia, K., Moreno, H., Ferrer, I., Behrens, C., Cuadrado, M., Paz-Ares, L., Bustelo, X.R., Gil-Bazo, I., Alameda, D., Lecanda, F., Calvo, A., Agorreta, J., 2019. Am. J. Respir. Crit. Care Med. 200, 888–899.
Gong, H.-Y., Wang, Y., Han, G., Song, Q.-B., 2019. Thoracic Cancer 10, 1136–1140.
Hill, M.G., Kelley, S.O., 2008. Bioinorganic Electrochemistry. Springer Netherlands, pp. 129–160.
Jain, S., Lin, S.Y., Song, W., Su, Y.-H., 2019. Genet. Test. Mol. Biomarkers 23, 277–283.
Jayanthi, V., Das, A., Saxena, U., 2019. RSC Adv. 9, 16738–16745.
Jing, A., Xu, Q., Feng, W., Liang, G., 2020. Micromachines 11, E660.
Khanmohammadi, A., Ghazizadeh, A., Hashemi, P., Afkhami, A., Arduini, F., Bagheri, H., 2020. J. Iran. Chem. Soc. 17.
Layqah, L.A., Eissa, S., 2019. Mikrochim. Acta 186, 224.
Liv, L., 2021. Microchem. J. 168, 106445. Devoted to the Application of Microtechniques in All Branches of Science.
Lv, H., Li, Y., Zhang, X., Gao, Z., Zhang, C., Zhang, S., Dong, Y., 2018. Biosens. Bioelectron. 112, 1–7.
Michela, B., 2021. Diagnostics 11, 1391.
Morales, M.A., Halpern, J.M., 2018. G Bioconjugate Chemistry 29, 3231–3239.
Patel, A., Patel, S., Patel, P., Tanavde, V., 2022. Front. Oncol. 12.
Redin, E., Garmendia, I., Lozano, T., Serrano, D., Senent, Y., Redrado, M., Villalba, M., De Andrea, C.E., Exposito, F., Ajona, D., Ortiz-Espinosa, S., Remirez, A., Bertolo, C., Sainz, C., Garcia-Pedrero, J., Pio, R., Lasarte, J., Agorreta, J., Montuenga, L.M., Calvo, A., 2021. Journal for Immunotherapy of Cancer 9, e001496.
Sabahi, A., Salahandish, R., Ghaffarinejad, A., Omidinia, E., 2020. Talanta 209, 120595.
Saeed, A.A., Sánchez, J.L.A., O'Sullivan, C.K., Abbas, M.N., 2017. Bioelectrochemistry 118, 91–99 (Amsterdam, Netherlands).
Senel, M., Dervisevic, M., Kokkokoğlu, F., 2019. Anal. Bioanal. Chem. 411, 2925–2935.
Seijo, L.M., Peled, N., Ajona, D., Boeri, M., Field, J.K., Sozzi, G., Pio, R., Zulueta, J.J., Spira, A., Massion, P.P., Mazzone, P.J., Montuenga, L.M., 2019. J. Thorac. Oncol. 14, 343–357.
Shoja, Y., Kermanpur, A., Karimzadeh, F., 2018. Biosens. Bioelectron. 113, 108–115.
Takeda, T., Yamamoto, H., Kanzaki, H., Suzawa, K., Yoshioka, T., Tomida, S., Cui, X., Murali, R., Namba, K., Sato, H., Torigoe, H., Watanabe, M., Shien, K., Soh, J., Asano, H., Tsukuda, K., Kitamura, Y., Miyoshi, S., Sendo, T., Toyooka, S., 2017. PLoS One 12, e0171356.
Tian, L., Liu, L., Li, Y., Wei, Q., Cao, W., 2016. Sci. Rep. 6, 30849.
Tran, L.T., Tran, T.Q., Ho, H.P., Chu, X.T., Mai, T.A., 2019. J. Nanomater. 2019, 1–9.
Travis, W.D., 2012. Modern Pathol. 25 (1). Article 1.
Wang, Z., Yang, H., Luo, S., Liu, B., Zhang, N., Li, L., Zhou, S., Shen, R., Xie, X., 2017. Lung Cancer 112, 1–9 (Amsterdam, Netherlands).
Yakoh, A., Pinyorospathum, C., Siangproh, W., Chailapakul, O., 2015. Sensors 15, 21427–21477.
Zhang, C., Zhang, S., Jia, Y., Li, Y., Wang, P., Liu, Q., Xu, Z., Li, X., Dong, Y., 2019. Biosens. Bioelectron. 126, 785–791.
Zhao, L., Kong, D., Wu, Z., Liu, G., Gao, Y., Yan, X., Liu, F., Liu, X., Wang, C., Cui, J., Lu, G., 2020. Microchem. J. 155, 104675.